



## Geologically distinct crude oils cause a common cardiotoxicity syndrome in developing zebrafish



Jee-Hyun Jung<sup>a</sup>, Corinne E. Hicken<sup>b</sup>, Daryle Boyd<sup>c</sup>, Bernadita F. Anulacion<sup>c</sup>, Mark G. Carls<sup>d</sup>, Won Joon Shim<sup>a</sup>, John P. Incardona<sup>c,\*</sup>

<sup>a</sup> Oil and POPs Research Group, Korea Institute of Ocean Science & Technology, 391 Jangmok-ri Jangmok-Myon, Geoje 656-830, Republic of Korea

<sup>b</sup> University of Alaska–Fairbanks Juneau Center, UAF Fisheries Division, 17101 Point Lena Loop Rd., Juneau, AK 99801, United States

<sup>c</sup> Environmental Conservation Division, Northwest Fisheries Science Center, National Oceanic and Atmospheric Administration, 2725 Montlake Blvd. E, Seattle, WA 98112, United States

<sup>d</sup> Auke Bay Laboratories, Alaska Fisheries Science Center, National Oceanic and Atmospheric Administration, 17109 Point Lena Loop Rd., Juneau, AK 99801, United States

### HIGHLIGHTS

- ▶ Crude oils from distinct geological sources produce an overlapping cardiotoxicity syndrome in developing zebrafish embryos.
- ▶ The patterns of AHR activation in cardiac tissue depended on the degree of weathering of the oils.
- ▶ Mechanisms of cardiotoxicity of petrogenic PAH mixtures likely shift with changes in mixture composition due to weathering.
- ▶ Data collected on intensively studied crude oils such as ANSCO can help predict the impacts of other oil spills.

### ARTICLE INFO

#### Article history:

Received 13 June 2012  
Received in revised form 8 December 2012  
Accepted 3 January 2013  
Available online 5 March 2013

#### Keywords:

Oil spills  
Marine pollution  
Fish embryology  
Developmental toxicity  
Cardiovascular toxicity

### ABSTRACT

Crude oils from different geological formations vary in composition, yet most crude oils contain a polycyclic aromatic hydrocarbon (PAH) fraction that would be expected to produce cardiotoxic effects in developing fish. To determine whether different crude oils or PAH compositions produce common or distinct effects, we used zebrafish embryos to directly compare two crude oils at different states of weathering. Iranian heavy crude oil (IHCO) spilled in the Yellow Sea following the 2007 Hebei Spirit accident was compared to the intensively studied Alaska North Slope crude oil (ANSKO) using two different exposure methods, water-accommodated fractions containing dispersed oil microdroplets and oiled gravel effluent. Overall, both crude oils produced a largely overlapping suite of defects, marked by the well-known effects of PAH exposure on cardiac function. Specific cardiotoxicity phenotypes were nearly identical between the two oils, including impacts on ventricular contractility and looping of the cardiac chambers. However, with increased weathering, tissue-specific patterns of aryl hydrocarbon receptor (AHR) activation in the heart changed, with myocardial AHR activation evident when alkyl-PAHs dominated the mixture. Our findings suggest that mechanisms of cardiotoxicity may shift from a predominantly AHR-independent mode during early weathering to a multiple pathway or synergistic mode with prolonged weathering and increased proportions of dissolved alkyl-PAHs. Despite continued need for comparisons of crude oils from different sources, the results here indicate that the body of knowledge already acquired from studies of ANSCO is directly relevant to understanding the impacts of other crude oil spills on the early life history stages of fish.

Published by Elsevier Ltd.

### 1. Introduction

Systematic comparison of toxic responses to different crude oils could help guide and expedite assessment of recent and future

spills. Crude oils from different origins have distinct chemical compositions (Stout and Wang, 2007), hence potentially differing toxicity. A few studies compared the general toxicity (e.g. LC50s) of different types of crude oils and refinery products in aquatic

**Abbreviations:** AHR, aryl hydrocarbon receptor; ANSCO, Alaska North Slope crude oil; BTEX, benzene, toluene, ethylbenzene, xylene; CYP1A, cytochrome P4501A; HEWAF, high-energy water accommodated fraction; hpf, hours post fertilization; IHCO, Iranian heavy crude oil; OGE, oiled gravel effluent; PAHs, polycyclic aromatic hydrocarbons.

\* Corresponding author. Tel.: +1 206 860 3347.

E-mail address: [john.incardona@noaa.gov](mailto:john.incardona@noaa.gov) (J.P. Incardona).

species (Anderson et al., 1974; Neff et al., 2000). The most extensive information on the toxicity of crude oil to developing fish is derived from studies on Alaska North Slope crude oil (ANSCO), following the 1989 Exxon Valdez oil spill (Peterson, 2001). Those studies focused primarily on pink salmon (*Oncorhynchus gorbuscha*) and Pacific herring (*Clupea pallasii*), species impacted by the spill. More recent studies in our laboratory utilized the zebrafish model to dissect mechanisms of developmental toxicity associated with ANSCO and polycyclic aromatic hydrocarbons (PAHs) derived from crude oil and other pyrogenic sources (Incardona et al., 2004, 2005, 2006; Hicken et al., 2011; Incardona et al., 2011). Only a few other studies have examined the effects of geologically distinct crude oils on developing fish, and have focused on different species. This includes the effects of Mesa light and Bass Strait crude oils on mummichog (*Fundulus heteroclitus*) and rainbowfish (*Melanoaenia fluviatilis*), respectively (Couillard, 2002; Pollino and Holdway, 2002). While all of the aforementioned studies point to a common cardiovascular syndrome induced in developing teleost embryos following exposure to crude oil, there have been no systematic comparisons of different oil types using cardiotoxic endpoints, and in a species that is as tractable for mechanistic insight as zebrafish. Our studies in zebrafish indicate that functional and morphological impacts on the developing heart are among the most sensitive indicators of exposure to ANSCO (Carls et al., 2008; Carls and Meador, 2009; Incardona et al., 2009; Hicken et al., 2011). Identification of common mechanisms among other crude oils would be useful in terms of assessing oil spill impacts on the most sensitive and informative endpoints. Insights from past research on ANSCO could help guide and expedite the assessment of more recent oil spills, including the Deepwater Horizon incident, if the cardiotoxic effects of different crude oils to fish early life history stages are similar.

The Hebei Spirit oil spill occurred 7 December 2007 off the coast of South Korea, and was recorded as one of the largest tanker spills of recent years, comparable to the Prestige oil spill in 2002 and Tasman Spirit in 2003 (ITOPF, 2008). Three different kinds of crude oil (United Arab Emirates Upper Zakum, Kuwait export crude and Iranian heavy crude) were spilled. High waves (up to four meters) and northwesterly winds ( $10\text{--}14\text{ m s}^{-1}$ ) for several days after the spill led to widespread distribution and stranding of oil on the coastline of Taean County (Kim et al., 2010), a region rich in marine and coastal resources. Many marine species were found dead on rocky shores and beaches and more than 8571 ha of land-based fish aquaculture facilities were directly affected by the crude oil. Hatching success rate in rockfish and flatfish declined to less than 50% in land-based aquaculture facilities using water from spill zones (National Fisheries Research and Development Institute, Republic of Korea, unpublished data). This spill provided the opportunity to directly compare a Middle Eastern crude oil to ANSCO.

Previous studies on ANSCO demonstrated that toxicity to fish embryos increased (per unit mass of total PAHs) as weathering changed the composition of dissolved polycyclic aromatic hydrocarbons (PAHs) toward an enrichment of the tricyclic fluorenes, dibenzothiofenenes, and phenanthrenes (Carls et al., 1999; Heintz et al., 1999). Later studies comparing the toxicity of individual parent (non-alkylated) tricyclic PAHs to the toxicity of ANSCO using the zebrafish model showed that the oil-derived PAH mixture (with composition dominated by parent PAHs) produce defects in embryonic cardiac function that were not dependent on activation of aryl hydrocarbon receptors (AHRs) (Incardona et al., 2004, 2005). The AHR family comprises ligand-activated transcription factors that regulate the xenobiotic metabolic response to PAHs (i.e. AHR-mediated), primarily by activating the synthesis of cytochrome P4501A (CYP1A) (Nebert et al., 2004). Individual tricyclic PAHs and lightly weathered ANSCO were both cardiotoxic to zebrafish embryos without activation of AHR in myocardial cells (i.e. AHR-independent), as measured by

induction of CYP1A. In assays of single compounds, dibenzothiofene and phenanthrene appeared equipotent, while fluorene produced less severe impacts on cardiac function (Incardona et al., 2004). In contrast, some higher molecular weight PAHs (e.g. benz[a]anthracene) and retene, a C4-alkyl-phenanthrene, caused “dioxin-like” cardiotoxicity that is dependent on activation of the zebrafish AHR2 isoform and is associated with myocardial CYP1A induction (Incardona et al., 2006; Scott et al., 2011). The toxicity of different crude oils may thus depend on an interplay of these (and possibly other) mechanisms, and it is unclear whether simple additivity models for PAH toxicity (French-McCay, 2002; McGrath and Di Toro, 2009) or more complex models combining multiple modes of action (e.g. Barron et al., 2004) are relevant for predicting oil toxicity to fish early life history stages. This question is important for understanding oil spill impacts because different crude oils may contain different ratios of these families of tricyclic compounds. Also, the composition of dissolved PAHs shifts during weathering from dominance by parent compounds to dominance by alkylated compounds suggesting the possibility of a corresponding shift from AHR-independent to AHR-mediated cardiotoxicity.

To both identify the potential for long-term impacts of the Hebei Spirit spill, determine what assays would be best applied in more logistically difficult studies of marine fish, and expand our understanding of basic toxicity mechanisms of different crude oils, we used zebrafish embryos to directly compare the phenotypes associated with exposure to Iranian heavy crude oil (IHCO) from the Hebei Spirit hold to ANSCO. We used two very different methods to produce water with dissolved oil components: high-energy water-accommodated fractions (HEWAFs) and oiled-gravel generator columns (oiled gravel effluent, OGE). HEWAF preparations are designed to mimic the conditions of physical dispersion of oil droplets in an open ocean oil spill under high energy wave conditions, while OGEs are designed to mimic the slow time-release of dissolved PAHs during prolonged weathering of an oiled shoreline. The goals of these studies were to determine (1) if novel phenotypes were associated with exposure to IHCO, (2) whether the effects of IHCO on heart development were similar to ANSCO; (3) how cardiotoxicity might shift with changing PAH composition during weathering; and (4) whether the different crude oils might cause different tissue-specific patterns of CYP1A induction. These studies were not designed to determine thresholds for toxicity or  $EC_{50}$ s, and the focus was on the physiological (i.e. cardiac) responses of individual animals.

## 2. Materials and methods

### 2.1. Zebrafish exposure

A zebrafish breeding colony (wild type AB) was maintained using routine procedures (Linbo, 2009). Fertilized eggs were collected in water adjusted to a conductivity of approximately  $1500\text{--}1600\ \mu\text{S cm}^{-1}$ , pH 7.5–8 with Instant Ocean salts (“system water”). Fish were maintained and treated according to an IACUC-approved protocol and anesthetized with  $\sim 1\text{ mM MS-222}$ . HEWAFs were prepared by manual shaking in separatory funnels as previously described (Carls et al., 2008; Hatlen et al., 2010). The ANSCO was partially weathered artificially by slow heating until volume was reduced by 20% (Marty et al., 1997). For HEWAF preparations, IHCO and ANSCO were diluted 1:10000 into 100 mL system water (100 ppm oil mass load) and 1:20000 into 1 L system water (50 ppm oil mass load). Gravel was coated with IHCO at a loading of  $6\text{ g oil kg}^{-1}$  gravel by manually shaking in an uncoated stainless steel paint can, followed by air drying in a thin layer for 24 h prior to loading into a column. ANSCO oiled gravel ( $6\text{ g kg}^{-1}$ ) was similarly prepared for a prior study, and had been weathered with zebrafish

system water for one week before storage at  $-20^{\circ}\text{C}$  (Incardona et al., 2005). This gravel was reused for more prolonged weathering (Hicken et al., 2011). ANSCO and IHCO HEWAF exposures were carried out simultaneously either in 100-mm glass petri dishes with 2 replicates of 50 embryos in 25 mL for each treatment (100 ppm oil load), or in 60-mm glass petri dishes with 4 replicates of 20 embryos in 10 mL for each treatment. HEWAF exposures were carried out with dishes randomly distributed in an incubator held at  $28.5^{\circ}\text{C}$ . For gravel column effluent exposures, groups of 25 embryos were maintained in each of four open 60-mm glass petri dishes submerged in either control (CGE) or oiled gravel effluent (OGE) as described previously, with temperature held at  $28^{\circ}\text{C}$  with submersible aquarium heaters (Incardona et al., 2005). Zebrafish embryos were added to the IHCO effluents between days 2 and 4 of weathering (i.e. column flow), and again at day 53. Embryos were added to the ANSCO effluents on regular 2- to 4-day intervals from day 1 through day 51 of weathering. Data from time points not described here were previously published for the ANSCO exposure (Hicken et al., 2011). HEWAF exposures were initiated immediately after completion of the HEWAF preparation (no weathering). Embryos were exposed from early gastrulation (4–5 h post-fertilization, hpf) to either 48 hpf (long pec hatching stage) or 72 hpf (protruding mouth hatching stage; Kimmel et al., 1995). For the 100 ppm HEWAF and day 2–4 OGE exposures, embryos were scored at 48 hpf for defects, and a subset randomly selected for imaging. The remainder was allowed to continue incubation to 72 hpf. These developmental time points were chosen in order to make direct comparisons to previous studies on PAH effects on zebrafish heart development (Incardona et al., 2004, 2005, 2006), and observation of embryos throughout exposure showed that pericardial edema was first evident between 36 and 48 hpf. Any non-viable embryos (typically  $\leq 5\%$ ) were removed after initial overnight incubation. Column flow rates and temperature were monitored and embryos were observed daily.

## 2.2. Imaging of embryos

Embryos were manually dechorionated, observed, and imaged on a Nikon SMZ800 stereomicroscope or Zeiss Axioplan 2 compound microscope using a Fire-i 400 industrial video camera (Unibrain, San Ramon, CA) and BTV Pro software (Bensoftware.com) on Macintosh computers as previously described (Incardona et al., 2004, 2005). Pericardial edema and intracranial hemorrhage were scored as present or absent in live embryos. Heart rate was measured either by counting over a 10-s interval in live animals viewed on a stereomicroscope (day 53 OGE exposure), or by counting contractions in 10-s video clips (all other exposures). Severity of edema was quantified by measuring the pericardial area in left lateral images (collected on the stereoscope at  $63\times$  total magnification) using ImageJ ([rsbweb.nih.gov/ij/](http://rsbweb.nih.gov/ij/)) as described previously (Incardona et al., 2006). Edema accumulation was measured as increase in pericardial area by subtracting the average pericardial area measured in control embryos from all measures (controls and exposed), following conversion from pixels to  $\mu\text{m}^2$  based on a stage micrometer image. For the 100 ppm oil load HEWAF exposure, a subset of embryos were selected at random for imaging from each of the two replicates of 50 embryos. For the 50 ppm oil load HEWAF exposure, all 20 embryos from each replicate were imaged. For assessment of cardiac contractility, 5 embryos were randomly selected from 3 of the 4 replicates, mounted in 3% methylcellulose in the right lateral position (to better view the ventricle), and placed under a coverslip for viewing on the Zeiss Axioplan 2 with a  $20\times$  objective ( $200\times$  total magnification) with differential interference contrast optics, followed by collection of a pair of 5-s video clips focused on the ventricle and the atrium. Video files were opened in ImageJ and chamber dimensions measured in video frames corresponding to peak diastole and peak

systole along lines drawn at the same angle for each. Contractility was measured as fractional shortening with the formula (end-diastolic diameter minus end-systolic diameter)/end diastolic diameter (Bendig et al., 2006; Incardona et al., 2011). Dechorionated embryos were fixed in 4% phosphate-buffered paraformaldehyde and processed for immunofluorescence with anti-CYP1A (monoclonal antibody C10-7, Biosense Laboratories, Bergen, Norway) and anti-myosin heavy chain (monoclonal antibody MF20, Developmental Studies Hybridoma Bank, University of Iowa). Secondary antibodies (Invitrogen/Molecular Probes) were goat anti-mouse IgG<sub>3</sub> and goat anti-mouse IgG<sub>2b</sub>. Embryos were mounted in 3% methylcellulose and imaged using a Zeiss LSM 5 Pascal confocal system with Ar and HeNe lasers (Carl Zeiss Advanced Imaging).

## 2.3. Statistical analysis

Data were analyzed using JMP 6.0.2 for Macintosh. For phenotype occurrence data from the 50 ppm HEWAF exposure, a one-way ANOVA was applied to values from 4 replicates for each treatment. In a post hoc means comparison (Tukey–Kramer Honestly Significant Differences Test), there was no difference between IHCO- and ANSCO-exposed groups. For measures of pericardial area, cardiac chamber dimensions, and contractility, a nested ANOVA was used to test for a replicate “tank” effect (replicate nested under oil exposure) in addition to an effect of exposure. For pericardial area, ANOVA was applied to 20 measures from each of 4 replicates for HEWAFs and 6 (controls) or 11 (oil-exposed) measures from each of 2 replicates for OGE, while cardiac dimensions and contractility included 4 or 5 measures from each of 3 replicates. In the measurement of cardiac dimensions, 2 embryos from each of the 15 randomly selected IHCO and ANSCO-exposed groups displayed the atrioventricular toggling phenotype, in which both chambers are dilated. Because this is a phenotype that is distinct from the more frequent ventricular contractility phenotype, the values for these 4 animals were excluded from the statistical analysis for atrial and ventricular contractility (resulting in 2 of 3 replicates for oil-exposed groups having  $N = 4$  instead of  $N = 5$ ). There was also no significant difference between IHCO- and ANSCO-exposed groups in post hoc means comparisons for pericardial area and chamber dimensions. In exposures involving only two treatment groups (e.g. control gravel and IHCO gravel at 53 days), means were compared by a *t*-test.

## 2.4. PAH measurements

100-mL water samples were collected at the start and end of embryo incubations throughout the duration of column weathering, and immediately after HEWAF preparation. The water samples were extracted with dichloromethane after addition of internal standards and analyzed using GC/MS selected ion monitoring with additional monitoring for alkylated PAHs as described elsewhere (Short et al., 1996; Sloan et al., 2005; Hicken et al., 2011). A PAH spiked water blank and a method blank sample were analyzed concurrently with samples. The lower limits of quantification for PAHs ranged from 0.38 to  $1.1\text{ ng L}^{-1}$ . Values for  $\sum$ PAHs in the text include all measured values above the detection limits (listed in the legend to Fig. 1).

## 3. Results

### 3.1. PAH compositions of water-accommodated fractions (HEWAFs) and oiled gravel effluents (OGES)

The PAH composition of whole oil for IHCO and ANSCO were similar, but showed some key differences (Fig. 1A). IHCO had a

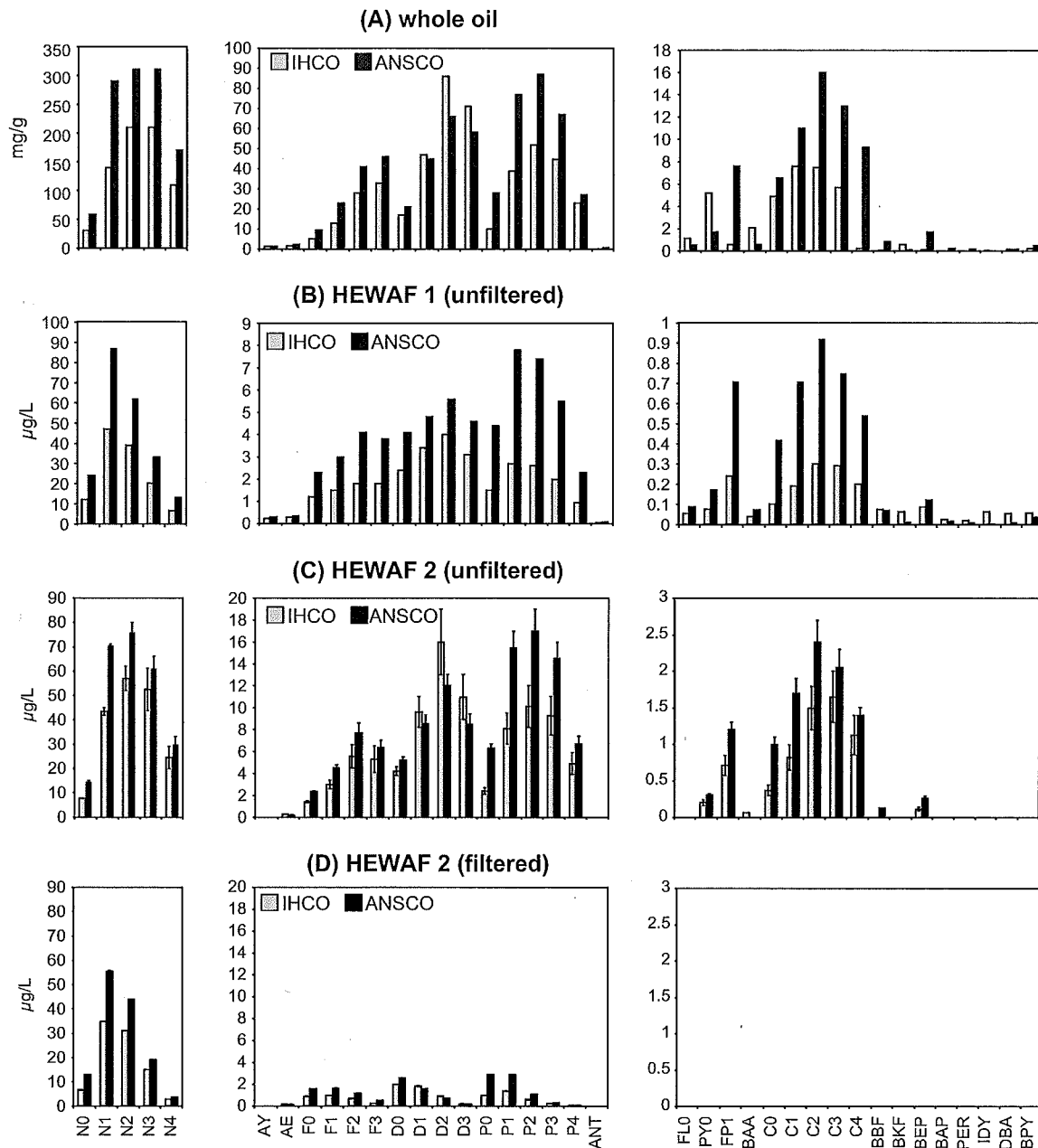


**Fig. 1.** PAHs concentrations in whole oil and HEWAF preparations at the start of exposure. Gray bars represent IHCO, black bars ANSCO. Values represent single measurements from the first HEWAF exposure, and means ( $\pm$ s.e.m.) for duplicate water samples from the second HEWAF exposure. (A) Whole oil. (B) Unfiltered HEWAF1 containing both dissolved PAH and oil droplets. (C) Unfiltered HEWAF2 containing both dissolved PAH and oil droplets. (D) Dissolved PAHs measured in filtered HEWAF2. N, naphthalenes; AY, acenaphthylene; AE, acenaphthene; F, fluorene; D, dibenzothiophene; P, phenanthrene; ANT, anthracene; FL, fluoranthene; PY, pyrene; FP, fluoranthenes/pyrenes; BAA, benz[a]anthracene; C, chrysene; BBF, benzo[b]fluoranthene; BKF, benzo[k]fluoranthene/benzo[k]fluoranthene; BEP, benzo[e]pyrene; BAP, benzo[a]pyrene; PER, perylene; IDY, indeno[1,2,3-cd]pyrene; DBA, dibenz[a,h]anthracene/dibenz[a,c]anthracene; BPY, benzo[ghi]perylene. Parent compound is indicated by a 0 (e.g., N0), while numbers of additional carbons (e.g. methyl groups) for alkylated homologs are indicated as N1, N2, etc.

slightly lower concentration of naphthalenes (37%), nearly half the level of phenanthrenes (48%), and slightly higher dibenzothiophenes (21%). Although embryos were exposed to unfiltered WAFs with PAH concentrations that appear relatively high (Fig. 1B and C), a previous study demonstrated that only the dissolved fraction contributes to toxicity (Carls et al., 2008). The total  $\sum$ PAHs for the first HEWAF preparations (HEWAF1, Fig. 1B) were  $158 \mu\text{g L}^{-1}$  and  $287 \mu\text{g L}^{-1}$  for IHCO and ANSCO, respectively, and  $284 \pm 37 \mu\text{g L}^{-1}$  and  $383 \pm 24 \mu\text{g L}^{-1}$ , respectively, for the second HEWAF preparations (HEWAF2, Fig. 1C). Analysis of PAHs in a filtrate of the second HEWAF preparation (HEWAF2, Fig. 1D) demonstrated that for IHCO

and ANSCO only 12% and 15%, respectively, of the total tricyclic PAHs (fluorenes, dibenzothiophenes, phenanthrenes) and 49% and 54%, respectively, of the more water-soluble naphthalenes were dissolved (dissolved  $\sum$ PAHs of  $102.7 \pm 0.2 \mu\text{g L}^{-1}$  and  $157.3 \pm 0.7$  for IHCO and ANSCO, respectively). Consistent with this, a water-washed, early weathering pattern of PAHs was present in the filtered fraction, with sets of parent-homolog series that sloped toward the right, (Fig. 1D) as opposed to the hump-shaped homolog series present in whole oils (Fig. 1A) or unfiltered HEWAFs (Fig. 1B and C). The filtered fraction was nearly completely representative of dissolved PAHs, indicated by the 98–99% lower

levels of the highly water insoluble phytane in the filtrates (from  $48.5 \pm 9.5 \mu\text{g L}^{-1}$  to  $0.073 \pm 0.011 \mu\text{g L}^{-1}$  for IHCO and  $26.5 \pm 3.5 \mu\text{g L}^{-1}$  to  $0.064 \pm 0.002 \mu\text{g L}^{-1}$  for ANSCO). Moreover, PAHs with 4 rings and higher were all below detection limits in the dissolved fraction (Fig. 1D). The higher relative levels of all compounds in the ANSCO HEWAFs are most likely due to more efficient mechanical dispersion than the heavier IHCO. Artificial pre-weathering of the ANSCO by heating primarily removes the highly volatile monoaromatic compounds (Marty et al., 1997). Because the IHCO was not pre-weathered in this manner, a key chemical difference between the ANSCO and IHCO HEWAFs would be the presence of these monoaromatic compounds (e.g. benzene, toluene, ethylbenzene, xylene; BTEX) in the latter.

OGEs contain no whole oil, and although the IHCO was fresh and the ANSCO was artificially weathered to remove BTEX, air-drying of gravel prior to packing in columns would eliminate BTEX from the IHCO gravel. Over time, the PAH composition of both OGEs changed as expected from previous weathering studies (Short and Heintz, 1997), with early time points dominated by parent (non-alkylated) PAHs, shifting to a pattern dominated by alkylated homologs at later time points (Fig. 2). This is reflected graphically by a shift from step-wise reductions toward the right within each homolog cluster (e.g. Fig. 2A, F0 through F3) to hump-shaped clusters or step-wise increases to the right within clusters (e.g. Fig 2C and D, D0 through D4 and F0 through F3, respectively). There were interesting differences in the patterns from IHCO compared to ANSCO, which may reflect the relationship between other physical–chemical properties of crude oils to the water-solubility of individual PAH classes. For example, although both oils were applied to the gravel at the same level ( $6 \text{ g kg}^{-1}$ ) and use the same flow rates, initial PAH concentrations were much higher for ANSCO (Figs. 2A and E). Moreover, while the initial ANSCO OGE was dominated by both parent dibenzothiophene (D0) and phenanthrene (P0) (Fig. 2A), minimally weathered IHCO OGE was dominated by parent dibenzothiophene (D0), but C1-phenanthrene (P1) instead of P0 (Fig. 2E). In addition, chrysenes C0–C3 were detected at low levels in all IHCO samples (Fig. 2E–G), but except for parent chrysene (C0), were below detection limits in most ANSCO samples, (Fig. 2B and D).

In summary, both exposure methods (HEWAF and OGE) produced a range of waterborne PAH concentrations and compositions, as well as exposures that allow the comparison of effects with and without the presence of BTEX.

### 3.2. Similarities and differences between the gross phenotypes of embryos exposed to IHCO or ANSCO

We compared the toxicity of IHCO and ANSCO in four independent assays. Two exposures were carried out with HEWAFs and two exposures were carried out with oiled gravel columns. The OGE exposures were performed with the same IHCO oiled gravel column run continuously, with embryo toxicity tested 50 days apart. The overall morphological impacts of exposure were assessed in one HEWAF exposure and both OGE exposures, while the second HEWAF exposure focused in more detail on specific aspects of cardiotoxicity. The collective suite of oil-associated defects was indistinguishable between embryos exposed to either IHCO HEWAF or OGE (Table 1 and Fig. 3). Pericardial edema was obvious by 48 hpf with exposure to ANSCO (Fig. 3B) and IHCO (Fig. 3C) HEWAF preps, as well as IHCO OGE (Fig. 3E; ANSCO OGE not shown). In both HEWAF and OGE exposures at early but not late time points, ANSCO caused pectoral finfold defects at a later developmental stage (i.e. 72 hpf, data not shown) as previously observed (Incardona et al., 2005). In contrast a different type of caudal finfold defect was observed by 48 hpf following IHCO exposure (Fig. 3C and E). This malformation was observed at an equivalently

high frequency (80%) in both HEWAF and OGE exposures and involved reduced outgrowth of the caudal finfold rays, often with a notch on either the dorsal or ventral side near the end of the notochord (e.g. Fig. 3E).

We quantified two common types of cardiovascular toxicity associated with embryonic exposure to crude oil in zebrafish, pericardial edema and intracranial hemorrhage. Both of these effects occurred at high frequency with both ANSCO and IHCO (Table 1) and with both types of exposures (HEWAF and OGE). Pericardial edema was also assessed by measuring the increase in pericardial area for embryos exposed simultaneously to either ANSCO or IHCO HEWAFs (50 ppm oil load), and the IHCO OGE (Fig. 4). Although the pericardial area was significantly increased relative to controls for all oil-exposed groups (ANOVA  $P < 0.0001$ ), there was no significant difference in the severity of edema between the different oil-exposed groups (Tukey–Kramer HSD post hoc test). Pericardial areas were increased by  $10.4 \pm 1.3 \mu\text{m}^2$  and  $12.5 \pm 2.6 \mu\text{m}^2$  in embryos exposed to IHCO HEWAF and OGE, respectively, and by  $10.4 \pm 1.2 \mu\text{m}^2$  in embryos exposed to ANSCO HEWAF, relative to controls (baseline pericardial areas of  $0 \pm 0.4$  and  $0 \pm 1.2$  in HEWAF and OGE controls, respectively). There was no replicate “tank” effect on pericardial area detected in a nested ANOVA ( $P = 0.2$ ).

In the second HEWAF exposure (50 ppm mass oil load), we also characterized the cardiotoxicity of both IHCO and ANSCO in more detail (Table 2). As described previously for ANSCO and individual tricyclic PAHs, there were a variety of cardiac function defects that occurred following exposure to either oil, but these were remarkably similar for each in both character and frequency. Embryos with edema most often had poorly looped hearts, scored as an inability to view a roughly circular, open atrioventricular canal in left lateral videos. Both IHCO and ANSCO HEWAFs had the same percentage of edematous embryos with poor looping ( $63\% \pm 4\%$  and  $63\% \pm 8\%$ , respectively). Embryos with and without poor looping most often also displayed reduced ventricular contractility, visible as stiff motion in video clips (Movie S1) and quantified as reduced fractional shortening, an indicator of systolic contractile function normalized to the diastolic (relaxed) diameter of the chambers (Bendig et al., 2006). This effect was specific to the ventricle, which displayed a reduced end-diastolic diameter (indicative of incomplete relaxation), while atrial dimensions and contractility were not different from controls (Table 2). While ventricles in controls had an average end-diastolic diameter of  $82.5 \pm 1.5 \mu\text{m}$ , ventricular diastolic diameters were reduced by 8–9% in IHCO-exposed ( $76.0 \pm 2.8 \mu\text{m}$ ) and ANSCO-exposed ( $75.4 \pm 2.5 \mu\text{m}$ ) embryos. A smaller proportion of embryos exposed to either IHCO ( $11\% \pm 2\%$ ) or ANSCO ( $19\% \pm 2\%$ ) displayed an atrioventricular “toggling” phenotype that appeared to be associated with blockage of the ventricular outflow tract. These embryos showed no circulating blood cells, with sequential contractions leading to forward and retrograde toggling of a bolus of blood cells between dilated ventricular and atrial chambers (Movie S2). In these cases, both chambers were demonstrably dilated, with end-diastolic diameters significantly higher than controls (Table 2). The higher frequency of this phenotype with ANSCO exposure was moderately significant ( $P = 0.06$ ), and may be related to the higher levels of tricyclic PAHs, especially parent compounds (Table S1).

We also measured heart rates in embryos exposed to ANSCO and IHCO HEWAFs, and IHCO OGE (Table S2). There was no effect on heart rate following exposure to HEWAFs of either oil type. Embryos exposed to IHCO OGE during initial column flow (relatively unweathered) also showed no difference in heart rate from controls, but embryos exposed to extensively weathered OGE at day 53 of column flow showed a significantly reduced heart rate (bradycardia), at 86% of the control rate ( $154 \pm 3$  vs.  $179 \pm 5$  beats  $\text{min}^{-1}$ ).

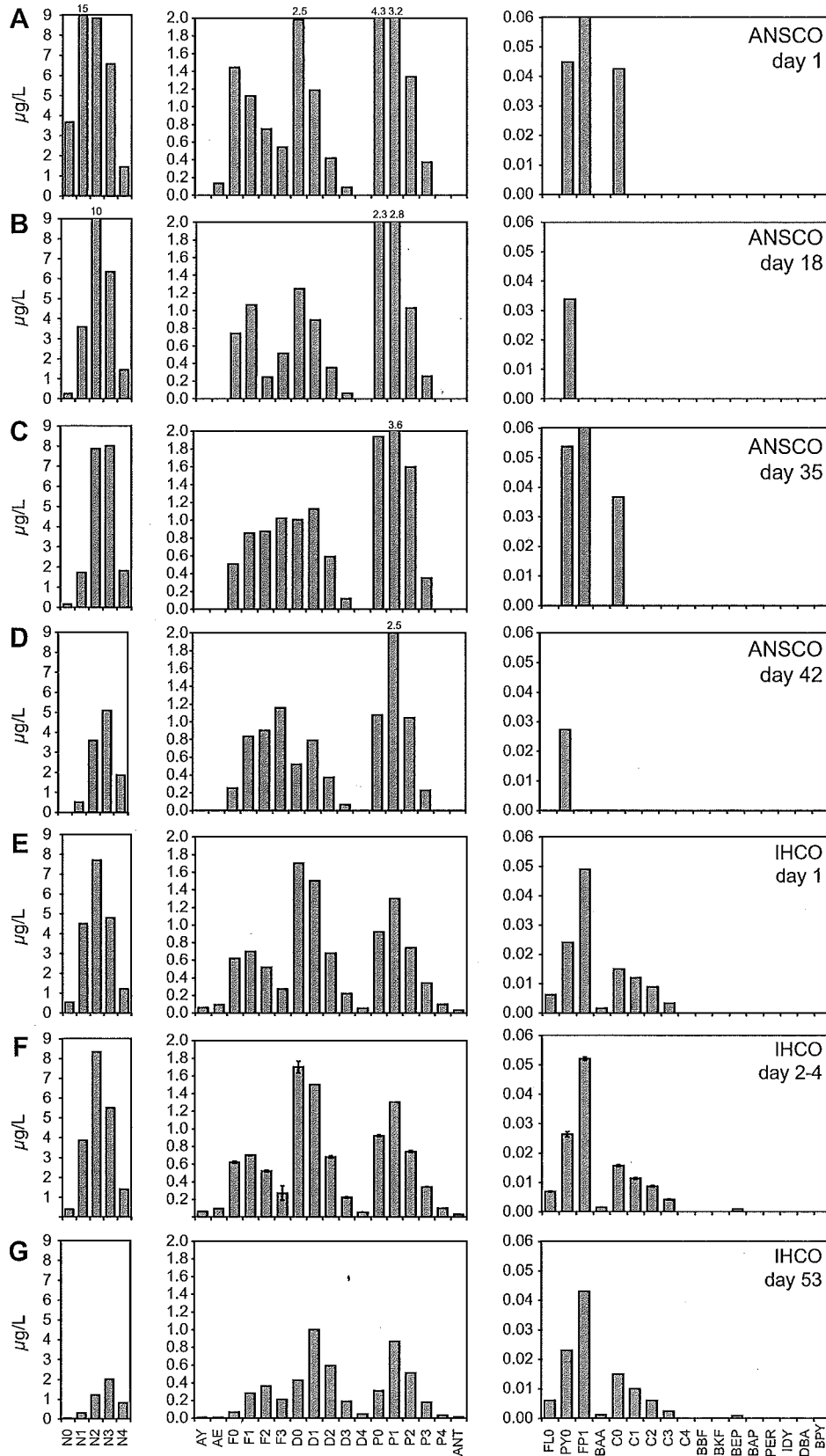


Fig. 2. PAH compositions of ANSCO and IHCO OGEs at different weathering time points. Values represent exposures for which toxicity data is presented in Table 1, or for which CYP1A immunofluorescence was assessed (Fig. 5). Data for ANSCO are from single measurements for column flow day 1 (A), day 18 (B), day 35 (C), and day 42 (D). Data for IHCO represent (E) single measurement from column flow day 1, (F) mean  $\pm$  s.e.m. of three measurements taken on days 2–4, and (G) single measurement from day 53. Abbreviations are the same as Fig. 1.

**Table 1**  
Gross morphological defects in embryos exposed to IHCO or ANSCO.<sup>a</sup>

Endpoint	Control	IHCO HEWAF (%) <sup>b</sup>	ANSCO HEWAF (%)	IHCO OGE day 4 (%)	ANSCO OGE day 44 (%)	IHCO OGE day 53 (%)
Pericardial edema	0	63	86	65	34	25
Intracranial hemorrhage	0	38	63	38	19	0
Tail malformation	0	80	0	80	0	0

<sup>a</sup> Occurrence data were obtained from roughly 100 embryos in each assay, except for IHCO OGE at day 53, *N* = 20.

<sup>b</sup> Data are for HEWAF1.

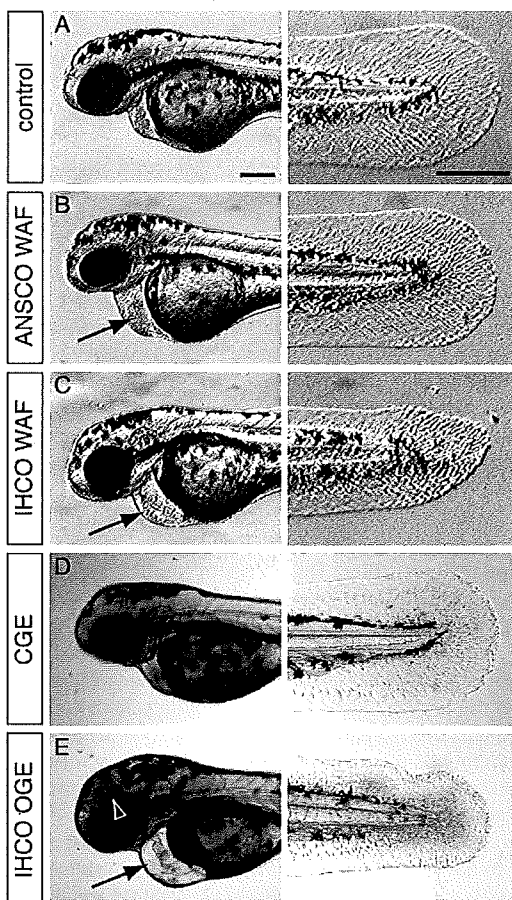


**Fig. 3.** Gross morphological effects of exposure to ANSCO or IHCO. Embryos were exposed from 4 hpf to 48 hpf and imaged live. (A) Embryo exposed to clean system water used to make HEWAFs. Embryos exposed to HEWAFs of ANSCO (B) or IHCO (C). (D) Embryo exposed to clean gravel effluent. (E) Embryo exposed to IHCO oiled gravel effluent. Images are representative of 40–60 embryos per treatment. Pericardial edema is indicated by arrows (B, C and E) and intracranial hemorrhage is indicated by the white arrowhead (E). Scale bars are 100  $\mu$ m.

### 3.3. Distinct patterns of CYP1A induction associated with different PAH compositions

Exposure to both crude oils produced very similar patterns of CYP1A induction overall, with some key differences. Consistent with previous studies, there was strong CYP1A immunofluorescence in the epidermis after exposure to either HEWAF (Fig. S1) or OGE (Fig. S2) from both ANSCO and IHCO, while control embryos showed only weak CYP1A immunofluorescence in the vascular endothelium (Figs. S1A and S2G). The pattern of epidermal CYP1A immunofluorescence was indistinguishable for both HEWAF and OGE exposures, with virtually all cells expressing CYP1A with a scattering of individual cells with much higher relative signal (Fig. S1B and C; Fig. S2A–D). This pattern was similar at both

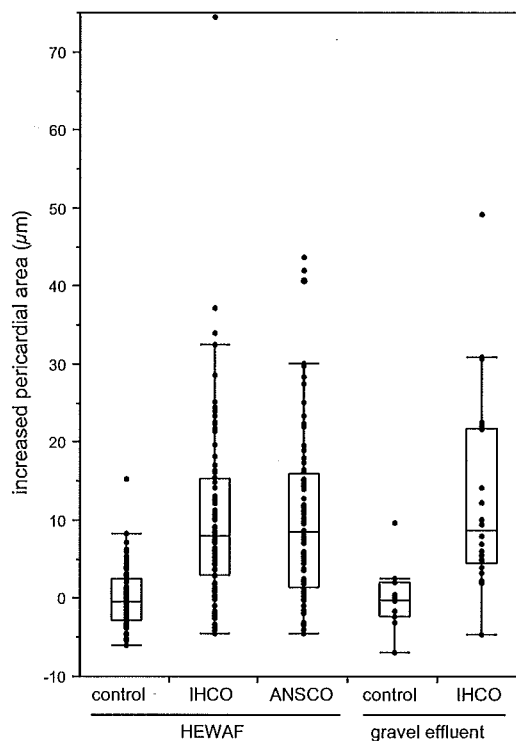


**Fig. 4.** Quantification of pericardial edema in embryos exposed to ANSCO or IHCO HEWAF, and IHCO OGE. Pericardial area was measured in lateral images of methylcellulose-mounted embryos, which were a randomly selected subsample (*N* is number of embryos measured per treatment). Box-and-whisker plots encompass the distribution of individual data points, with the mean indicated by the wider heavy line, the ends of the boxes 25th and 75th quartiles, and the ends of the whiskers encompassing the upper and lower quartiles  $\pm$  (1.5  $\times$  interquartile range). Data points outside the whiskers are potential outliers. ANOVA showed a significant effect of oil exposure ( $P < 0.001$ ).

48 hpf (Fig. S2A and B) and 72 hpf (Fig. S2C and D). Exposure to either ANSCO or IHCO OGE resulted in CYP1A induction in the endothelium of the trunk vasculature (Fig. S2E and F). These overall patterns of epidermal and peripheral vascular CYP1A induction did not change over the course of weathering (data not shown).

In contrast to the similar patterns of epidermal and trunk vascular CYP1A induction, the pattern of CYP1A induction in the heart changed over time during weathering of the columns (Fig. 5). Exposure to either ANSCO or IHCO OGE at early time points (days 14–16 and days 2–4, respectively) where dissolved PAHs were dominated by parent compounds (Figs. 2B and E) resulted in neither endocardial nor myocardial CYP1A immunofluorescence at either 48 or 72 hpf (Fig. 5A, D and E). By day 21 of column flow, ANSCO OGE exposure resulted in endocardial but not myocardial CYP1A induction (data not shown), but by day 35 (data not shown) and more so by day 42, exposure to ANSCO caused myocardial CYP1A induction evident at 48 hpf and more strongly at 72 hpf (Fig. 5B and C, arrowheads), in addition to strong endocardial CYP1A immunofluorescence at both 48 and 72 hpf (Fig. 5B and C,

**Table 2**  
Cardiac function in embryos exposed to IHCO or ANSCO HEWAFs from 5 to 48 hpf.

Cardiac measure	Control	IHCO	ANSCO	P value <sup>a</sup>
Edema (occurrence, %)	4 ± 1	70 ± 4	66 ± 7	<0.0001
Poor looping (occurrence, %)	6 ± 1	44 ± 2	40 ± 3	<0.0001
AV "toggle" (occurrence, %)	0	11 ± 2	19 ± 2	0.0003
Atrial diastolic diameter (μm)	84.7 ± 2.4	95.3 ± 5.2	92.1 ± 4.3	0.3
Atrial systolic diameter (μm)	64.3 ± 2.0	69.7 ± 3.2	67.8 ± 2.5	0.4
Ventricular diastolic diameter (μm)	82.5 ± 1.5	76.0 ± 2.8	75.4 ± 2.5	0.05 <sup>b</sup>
Ventricular systolic diameter (μm)	63.9 ± 1.3	66.0 ± 1.8	63.4 ± 1.7	0.5
Atrial contractility (%)	24.1 ± 1.2	25.9 ± 2.3	25.9 ± 1.7	0.6
Ventricular contractility (%)	22.4 ± 1.4	12.7 ± 1.5	15.5 ± 1.9	0.0008 <sup>b</sup>
Atrial diastolic diameter (μm) <sup>c</sup>	84.7 ± 2.4	124.3 ± 6.8	123.6 ± 1.9	0.001
Ventricular diastolic diameter (μm) <sup>b</sup>	82.5 ± 1.5	122.9 ± 3.2	140.6 ± 18.2	0.01

<sup>a</sup> Occurrence of phenotypes was assessed in 80 embryos for each treatment (4 replicates of 20); cardiac chamber dimensions were obtained from 15 embryos randomly selected from each of 3 replicates (5 per replicate, 3 replicates randomly selected from the 4 above). Data were analyzed by ANOVA with replicate nested within treatment to determine the presence of a "tank" effect. P values shown are for effects of oil exposure.

<sup>b</sup> No effect of replicate (e.g. "tank" effect) in nested ANOVA: ventricular diastolic diameter,  $P = 0.3$ ; ventricular contractility,  $P = 0.9$ .

<sup>c</sup> Chamber dimensions measured in oil-exposed embryos with "toggle" phenotype, obtained from two individuals each for IHCO and ANSCO exposures from the 15 randomly selected for chamber measurements. Measures for both IHCO and ANSCO were pooled into a "toggle phenotype" group for statistical comparison to controls by a *t*-test.

arrows). Myocardial CYP1A induction was observed by confocal microscopy in 5/9 individuals examined for the exposure starting on day 35, and in 7/7 individuals from the exposure starting on day 42.

#### 4. Discussion

We previously showed that exposure of zebrafish embryos to ANSCO produced the same suite of defects whether achieved by HEWAF or OGE (Incardona et al., 2005; Carls et al., 2008). Overall, we observed strikingly similar results here with IHCO, with nearly identical cardiac phenotypes following exposures to HEWAFs of either oil type. Using both exposure methods, IHCO produced a developmental toxicity syndrome that largely overlaps that of ANSCO, primarily characterized by impacts on the developing heart that become apparent between 36 and 48 hpf in zebrafish. In particular, the HEWAF method produced similar PAH compositions from both crude oils, which caused essentially identical, specific effects on cardiac function. The second HEWAF preparation produced dissolved PAH concentrations that were typical of early weathering, with higher concentrations of parent over alkylated tricyclic compounds, and both IHCO and ANSCO HEWAFs resulted in reduced ventricular contractility and nearly identical morphological impacts on the developing heart. Although neither the underlying mechanism nor the chemical etiology is yet known, both crude oils also produced a high frequency of intracranial hemorrhage, consistent with transient disruption of vascular stability during a key phase of vasculogenesis in the developing brain (Liu et al., 2007; Buchner et al., 2007). Thus the most overt types of toxicity associated with ANSCO are found in a heavy crude oil of different character, indicating considerable overlap in biologically active chemical components. On the other hand, a distinct chemical component of IHCO is evident from the high frequency of tail defects observed as early as 48 hpf, while we did not observe the type of pectoral fin-fold defects characteristic of ANSCO exposure at 72 hpf. These findings attest to the chemical complexity of crude oils and the need for a more detailed analysis that includes both an expanded biological focus as well as characterization of other chemical constituents besides the conventionally measured PAHs. Nevertheless, at lower concentrations and more prolonged weathering for both oils, fin defects are not observed while pericardial edema persists.

That similar phenotypes are produced by two very different exposure methods has important implications for the relationship between crude oil chemical composition and developmental toxic-

ity in fish. HEWAF preparations contain mechanically dispersed oil droplets, while the effluent of oiled gravel generator columns contain only oil constituents that are soluble in water. The pattern of CYP1A induction in the epidermis, the tissue in direct contact with aqueous PAHs or whole oil droplets, was identical between HEWAF and OGE exposures, strongly suggesting similar toxicokinetics between the water-soluble components of both preparations. This is entirely consistent with previous interpretations that whole oil is not required for toxicity and that toxicity stems solely from compounds that are available by dissolution in water (reviewed by Carls and Meador, 2009). On a basis of total  $\Sigma$ PAH, it may appear that the HEWAF preparations are less toxic than OGEs; HEWAFs showed comparable toxicity at a higher total  $\Sigma$ PAH. This is largely due to the much higher levels of naphthalenes in the HEWAFs, whereas each exposure method produced much more comparable levels of the tricyclic PAHs. Thus, the findings here confirm and extend conclusions from previous studies that as oil weathers and 2-ring compounds are depleted, toxicity to fish embryos increases per unit mass of PAH as the tricyclic compounds begin to dominate the composition (Carls et al., 1999; Heintz et al., 1999; Carls and Meador, 2009). On this basis, the HEWAFs and OGE would be expected to have comparable potency. The comparable effects of HEWAFs with and without BTEX (IHCO vs. ANSCO) are also consistent with other studies demonstrating that toxicity to fish embryos is derived from less volatile PAHs, with no contribution from BTEX (Marty et al., 1997).

Despite the overall similarity in toxicity syndrome induced by ANSCO and IHCO, our findings suggest that, on a more detailed level, (1) cardiac impacts can arise from multiple mechanisms that may differentially involve the AHR, and (2) there is a balance of mechanisms that shift during weathering, dependent on PAH composition. This complexity is indicated by the changing influence of weathering on heart rate impacts, the shifting patterns of CYP1A induction in cardiac tissues, and specific aspects of cardiac phenotypes, e.g. the higher frequency of the AV toggling phenotype that may be associated with higher concentrations of parent tricyclic PAHs. In an earlier study (Incardona et al., 2005), we assessed the effects of AHR knockdown in exposure to OGE only up to 7 days of column flow, which produced a PAH composition dominated by the more water-soluble parent PAHs (comparable to the day 1 sample used here and the second HEWAF preparations). The studies here are a direct extension of the 2005 study, because we used the same gravel, but assessed the OGE at much later stages of weathering. In the former, CYP1A induction was observed in the endocardium only, and not the myocardium. In all cases where

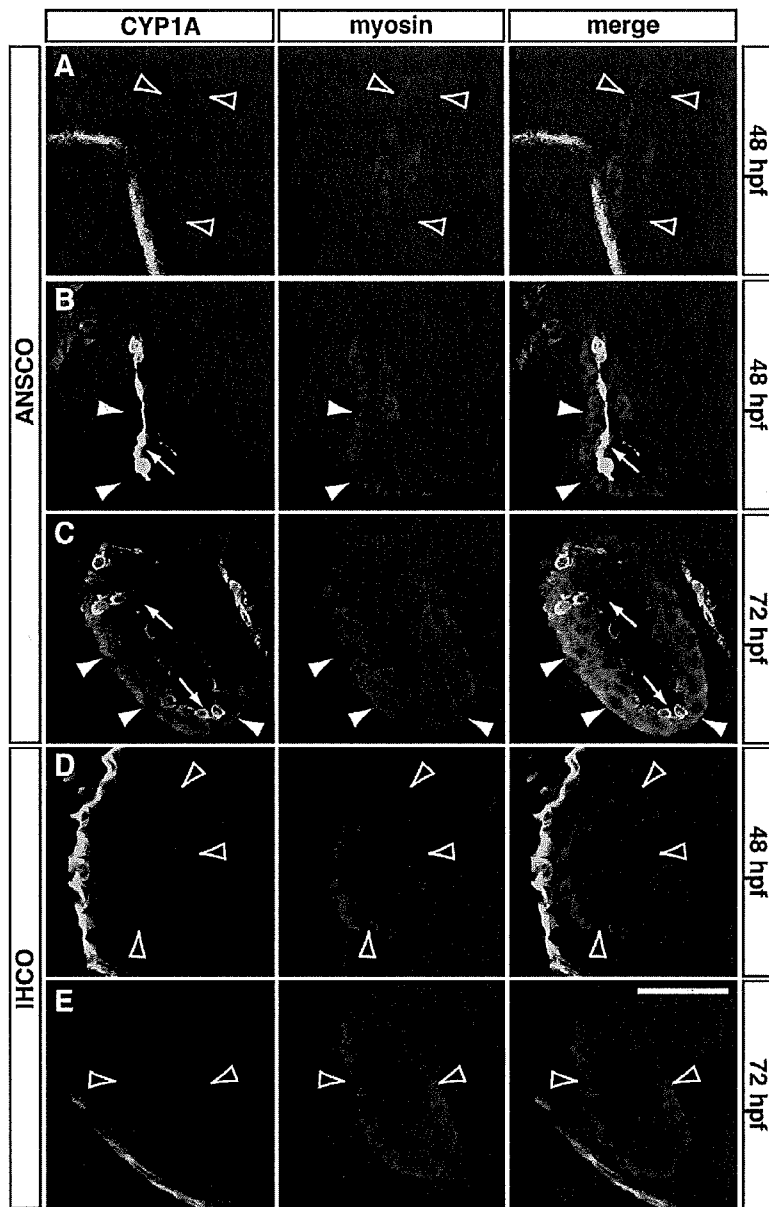


**Fig. 5.** Differential induction of CYP1A in cardiac tissue in fresh IHCO OGE and weathered ANSCO OGE. Embryos were exposed to OGEs from 4 hpf to 48 and 72 hpf, then fixed and processed for CYP1A (green) and myosin heavy chain (red, marking cardiomyocytes) immunofluorescence. Confocal optical sections show embryos exposed to ANSCO (A–C) or IHCO (D and E), with anterior to left and dorsal at top. Filled arrowheads indicate CYP1A<sup>+</sup> myocardial cells, smaller arrows indicate CYP1A<sup>+</sup> endocardial cells (A and B). Unfilled arrowheads indicate myocardial cells lacking CYP1A immunofluorescence. Exposure time points in terms of weathering were (A) days 14–16, (B and C) days 42–45, and (D and E) days 1–4. Scale bars are 50  $\mu$ m. Images are representative of 7–12 embryos examined for each treatment.

individual PAH compounds cause AHR-dependent cardiotoxicity, we observed that myocardial AHR activation (indicated by CYP1A induction) is necessary for toxicity (e.g. benz[a]anthracene, retene, benzo[a]pyrene; Incardona et al., 2006, 2011; Scott et al., 2011). Conversely, in these collective studies of twelve different individual PAHs, we have not observed myocardial CYP1A induction without concomitant defects in heart development. Although we did not perform knock-down studies with AHR morpholinos, the observation of myocardial CYP1A induction at both 48 and 72 hpf in embryos exposed to ANSCO columns after 40 days of weathering is most likely indicative of pathologically effective AHR activation. In other words, we have not observed myocardial CYP1A activation without demonstrable cardiotoxicity. As observed for ANSCO columns during early weathering (here and Incardona et al., 2005),

embryos exposed to IHCO OGE showed marked cardiotoxicity, but no myocardial AHR activation.

Overall these findings show that two crude oils from distinct geological sources produce similar syndromes that are dominated by cardiac dysfunction. However, the weathering state of dissolved PAHs may determine the predominance of what is likely to be several distinct cardiotoxic mechanisms. Our cumulative zebrafish studies indicate that, irrespective of mechanism, gross cardiotoxic endpoints based on morphology (e.g. edema, looping) should be very sensitive for assessing injury thresholds (e.g. EC<sub>50S</sub>) in marine species for crude oils from different geographical regions, using dose–response studies that model either an open-water (HEWAF) or shoreline (OGE) oil spill. On the other hand, our findings here suggest that a changing balance of mechanisms with weathering

will complicate the development of potentially more sensitive molecular indicators of petroleum cardiotoxicity. Finally, while there is value in continued comparisons of crude oils from a wider range of sources, our results also indicate that the large body of knowledge acquired from the study of ANSCO is applicable to future impact assessments for spills involving other sources of crude oil.

### Acknowledgements

The authors thank Tiffany Linbo for zebrafish husbandry, Heather Day for technical assistance, Marie Larsen and Larry Holland for analysis of PAHs in ANSCO oiled gravel effluent, and Richard Edmunds and Nat Scholz for critical review of the manuscript. These studies were funded in part by the NOAA Coastal Storms Program and Oceans and Human Health Initiative, and grants to W.J.S. from the Korean Ministry of Land, Transport and Maritime Affairs (PM56951: Oil Spill Environmental Impact Assessment and Environmental Restoration, and PE99151).

### Appendix A. Supplementary material

Supplementary data associated with this article can be found, in the online version, at <http://dx.doi.org/10.1016/j.chemosphere.2013.01.019>.

### References

- Anderson, J.W., Neff, J.M., Cox, B.A., Tatem, H.E., Hightower, G.M., 1974. Characteristics of dispersions and water-soluble extracts of crude and refined oils and their toxicity to estuarine crustaceans and fish. *Mar. Biol.* 27, 75–88.
- Barron, M.G., Carls, M.G., Heintz, R., Rice, S.D., 2004. Evaluation of fish early life-stage toxicity models of chronic embryonic exposures to complex polycyclic aromatic hydrocarbon mixtures. *Toxicol. Sci.* 78, 60–67.
- Bendig, G., Grimmmer, M., Huttner, I.G., Wessels, G., Dahme, T., Just, S., Trano, N., Katus, H.A., Fishman, M.C., Rottbauer, W., 2006. Integrin-linked kinase, a novel component of the cardiac mechanical stretch sensor, controls contractility in the zebrafish heart. *Genes Dev.* 20, 2361–2372.
- Buchner, D.A., Su, F., Yamaoka, J.S., Kamei, M., Shavit, J.A., Barthel, L.K., McGee, B., Amigo, J.D., Kim, S., Hanosh, A.W., Jagadeeswaran, P., Goldman, D., Lawson, N.D., Raymond, P.A., Weinstein, B.M., Ginsburg, D., Lyons, S.E., 2007. Pak2a mutations cause cerebral hemorrhage in redhead zebrafish. *Proc. Natl. Acad. Sci. USA* 104, 13996–14001.
- Carls, M.G., Holland, L., Larsen, M., Collier, T.K., Scholz, N.L., Incardona, J.P., 2008. Fish embryos are damaged by dissolved PAHs, not oil particles. *Aquat. Toxicol.* 88, 121–127.
- Carls, M.G., Meador, J.P., 2009. A perspective on the toxicity of petrogenic PAHs to developing fish embryos related to environmental chemistry. *Human Ecol. Risk Assess.* 15, 1084–1098.
- Carls, M.G., Rice, S.D., Hose, J.E., 1999. Sensitivity of fish embryos to weathered crude oil: Part I. Low-level exposure during incubation causes malformations, genetic damage, and mortality in larval Pacific herring (*Clupea pallasii*). *Environ. Toxicol. Chem.* 18, 481–493.
- Couillard, C.M., 2002. A microscale test to measure petroleum oil toxicity to mummichog embryos. *Environ. Toxicol.* 17, 195–202.
- French-McCay, D.P., 2002. Development and application of an oil toxicity and exposure model. *OilToxEx. Environ. Toxicol. Chem.* 21, 2080–2094.
- Hatlen, K., Sloan, C.A., Burrows, D.G., Collier, T.K., Scholz, N.L., Incardona, J.P., 2010. Natural sunlight and residual fuel oils are an acutely lethal combination for fish embryos. *Aquat. Toxicol.* 99, 56–64.
- Heintz, R.A., Short, J.W., Rice, S.D., 1999. Sensitivity of fish embryos to weathered crude oil: Part II. Increased mortality of pink salmon (*Oncorhynchus gorbuscha*) embryos incubating downstream from weathered Exxon Valdez crude oil. *Environ. Toxicol. Chem.* 18, 494–503.
- Hicken, C.L., Linbo, T.L., Baldwin, D.H., Myers, M.S., Holland, L., Larsen, M., Scholz, N.L., Collier, T.K., Rice, G.S., Stekoll, M.S., Incardona, J.P., 2011. Sublethal exposure to crude oil during embryonic development alters cardiac morphology and reduces aerobic capacity in adult fish. *Proc. Natl. Acad. Sci. USA* 108, 7086–7090.
- Incardona, J.P., Carls, M.G., Day, H.L., Sloan, C.A., Bolton, J.L., Collier, T.K., Scholz, N.L., 2009. Cardiac arrhythmia is the primary response of embryonic Pacific herring (*Clupea pallasii*) exposed to crude oil during weathering. *Environ. Sci. Technol.* 43, 201–207.
- Incardona, J.P., Carls, M.G., Teraoka, H., Sloan, C.A., Collier, T.K., Scholz, N.L., 2005. Aryl hydrocarbon receptor-independent toxicity of weathered crude oil during fish development. *Environ. Health Perspect.* 113, 1755–1762.
- Incardona, J.P., Collier, T.K., Scholz, N.L., 2004. Defects in cardiac function precede morphological abnormalities in fish embryos exposed to polycyclic aromatic hydrocarbons. *Toxicol. Appl. Pharmacol.* 196, 191–205.
- Incardona, J.P., Day, H.L., Collier, T.K., Scholz, N.L., 2006. Developmental toxicity of 4-ring polycyclic aromatic hydrocarbons in zebrafish is differentially dependent on AH receptor isoforms and hepatic cytochrome P450 1A metabolism. *Toxicol. Appl. Pharmacol.* 217, 308–321.
- Incardona, J.P., Linbo, T.L., Scholz, N.L., 2011. Cardiac toxicity of 5-ring polycyclic aromatic hydrocarbons is differentially dependent on the aryl hydrocarbon receptor 2 isoform during zebrafish development. *Toxicol. Appl. Pharmacol.* 257, 242–249.
- I TOPF (International Tanker Owners Pollution Federation Limited), 2008. The environmental impact of the Hebei Spirit oil spill, Taean, South Korea. London, <<http://www.itopf.com/news-and-events/documents/HEBEISPIRIT-EnvironmentalImpact.pdf>>.
- Kim, M., Yim, U.H., Hong, S.H., Jung, J.-H., Choi, H.-W., An, J., Won, J., Shim, W.J., 2010. Hebei Spirit oil spill monitored on site by fluorometric detection of residual oil in coastal waters off Taean, Korea. *Mar. Pollut. Bull.* 60, 383–389.
- Kimmel, C.B., Ballard, W.W., Kimmel, S.R., Ullmann, B., Schilling, T.F., 1995. Stages of embryonic development of the zebrafish. *Dev. Dyn.* 203, 253–310.
- Linbo, T. L., 2009. Zebrafish (*Danio rerio*) husbandry and colony maintenance at the Northwest Fisheries Science Center. NOAA Technical Memorandum. US Department of Commerce, p 75.
- Liu, J., Fraser, S.D., Faloon, P.W., Rollins, E.L., Vom Berg, J., Starovic-Subota, O., Laliberte, A.L., Chen, J.-N., Serluca, F.C., Childs, S.J., 2007. A  $\beta$ Pix-Pak2a signaling pathway regulates cerebral vascular stability in zebrafish. *Proc. Natl. Acad. Sci. USA* 104, 13990–13995.
- Marty, G.D., Short, J.W., Dambach, D.M., Willits, N.H., Heintz, R.A., Rice, S.D., Stegeman, J.J., Hinton, D.E., 1997. Ascites, premature emergence, increased gonadal cell apoptosis, and cytochrome P4501A induction in pink salmon larvae continuously exposed to oil-contaminated gravel during development. *Can. J. Zool.-Rev. Can. Zool.* 75, 989–1007.
- McGrath, J.A., Di Toro, D.M., 2009. Validation of the target lipid model for toxicity assessment of residual petroleum constituents: monocyclic and polycyclic aromatic hydrocarbons. *Environ. Toxicol. Chem.* 28, 1130–1148.
- Nebert, D.W., Dalton, T.P., Okey, A.B., Gonzalez, F.J., 2004. Role of aryl hydrocarbon receptor-mediated induction of the CYP1 enzymes in environmental toxicity and cancer. *J. Biol. Chem.* 279, 23847–23850.
- Neff, J.M., Ostazeski, S., Gardiner, W., Stejskal, I., 2000. Effects of weathering on the toxicity of three offshore Australian crude oils and a diesel fuel to marine animals. *Environ. Toxicol. Chem.* 19, 1809–1821.
- Peterson, C.H., 2001. The “Exxon Valdez” oil spill in Alaska: acute indirect and chronic effects on the ecosystem. *Adv. Marine Biol.* 39, 1–103.
- Pollino, C.A., Holdway, D.A., 2002. Toxicity testing of crude oil and related compounds using early life stages of the crimson-spotted rainbowfish (*Melanotaenia fluviatilis*). *Ecotox. Environ. Safe.* 52, 180–189.
- Scott, J.A., Incardona, J.P., Pelkki, K., Shepardson, S., Hodson, P.V., 2011. AhR2-mediated; CYP1A-independent cardiovascular toxicity in zebrafish (*Danio rerio*) embryos exposed to retene. *Aquat. Toxicol.* 101, 165–174.
- Short, J.W., Heintz, R.A., 1997. Identification of Exxon Valdez oil in sediments and tissues from Prince William Sound and the Northwestern Gulf of Alaska based on a PAH weathering model. *Environ. Sci. Technol.* 31, 2375–2384.
- Short, J.W., Jackson, T.J., Larsen, M.L., Wade, T.L., 1996. Analytical methods used for the analysis of hydrocarbons in crude oil, tissues, sediments, and seawater collected for the natural resources damage assessment of the Exxon Valdez oil spill. *Amer. Fish. Soc. Symp.* 18, 140–148.
- Sloan, C.A., Brown, D.W., Pearce, R.W., Boyer, R.H., Bolton, J.L., Burrows, D.G., Herman, D.P., Krahn, M.M., 2005. Determining aromatic hydrocarbons and chlorinated hydrocarbons in sediments and tissues using accelerated solvent extraction and gas chromatography/mass spectrometry. In: Ostrander, G.K. (Ed.), *Tech. Aquatic Toxicol.*, vol. 2. CRC Press, Boca Raton, FL, pp. 631–651.
- Stout, S.A., Wang, Z., 2007. Chemical fingerprinting of spilled or discharged petroleum – methods and factors affecting petroleum fingerprints in the environment. In: Wang, Z., Stout, S.A. (Eds.), *Oil Spill Environmental Forensics*. Academic Press, London, pp. 1–53.